## **Activity-Suppressed Phase Separation**

Fernando Caballero\* and M. Cristina Marchetti® Department of Physics, University of California Santa Barbara, Santa Barbara, CA 93106

(Received 15 July 2022; accepted 1 December 2022; published 22 December 2022)

We use a continuum model to examine the effect of activity on a phase-separating mixture of an extensile active nematic and a passive fluid. We highlight the distinct role of (i) previously considered interfacial active stresses and (ii) bulk active stresses that couple to liquid crystalline degrees of freedom. Interfacial active stresses can arrest phase separation, as previously demonstrated. Bulk extensile active stresses can additionally strongly suppress phase separation by sustained self-stirring of the fluid, substantially reducing the size of the coexistence region in the temperature-concentration plane relative to that of the passive system. The phase-separated state is a dynamical emulsion of continuously splitting and merging droplets, as suggested by recent experiments. Using scaling analysis and simulations, we identify various regimes for the dependence of droplet size on activity. These results can provide a criterion for identifying the mechanisms responsible for arresting phase separation in experiments.

DOI: 10.1103/PhysRevLett.129.268002

Liquid-liquid phase separation (LLPS) occurs ubiquitously in biology and materials science. In this process, two immiscible fluids demix from a homogeneous state into two distinct liquids separated by soft interfaces. Recent attention has focused on LLPS in active systems [1,2]. Persistent motility is known to drive phase separation in systems in which the constituent particles have purely repulsive interactions through a process known as motilityinduced phase separation (MIPS) [3-5]. This is in contrast to equilibrium phase separation, which requires attractive interactions and occurs when attraction overcomes thermally driven entropic mixing. MIPS has been characterized extensively, experimentally, and theoretically, resulting in a detailed understanding of its underlying mechanisms [6], phases [7,8], critical properties [9], and laboratory realizations [10,11].

Less studied is the effect of activity on the phase diagram of fluid mixtures that do phase separate in equilibrium. Very recent experiments on immiscible phase-separating mixtures of active and passive fluids [12] have suggested that activity may both arrest phase separation, i.e., stabilize finite-size structures, preventing the system from reaching bulk phase separation, and also suppress it by shifting the critical temperature to lower values and reducing the region of the phase diagram where the two fluids are demixed. While binary mixtures of active and passive species have been studied and modeled before in different contexts [13– 17], an understanding of this suppression is still missing.

Equilibrium liquid-liquid phase separation is well described by a continuum theory in terms of a conserved concentration field  $\phi(\mathbf{r},t)$  with an underlying free energy quartic in  $\phi$  coupled to a flow with velocity field v [18]. Activity has been introduced in equilibrium models through the addition of time reversal symmetry breaking terms to the currents that drive the dynamics of the concentration field [19] and through interfacial stresses that describe activity-induced self-shearing of the interface [20,21]. It has been shown that these nonequilibrium mechanisms can arrest phase separation and stabilize finite-size droplets [21,22], but, as we see below, they do not change the critical temperature of the passive phaseseparating mixture.

In this Letter, we examine the effect of activity on a phase-separating mixture of a passive fluid and an active nematic and show that in this system, activity not only arrests phase separation, but can completely suppress it. The suppression originates from the presence of liquid crystalline degrees of freedom that generate bulk active stresses not present in scalar models. It is known that such active stresses destabilize the homogeneous nematic state on all scales [23], resulting in active turbulent dynamics. This yields a continuous local stirring that mixes the fluid into a uniform state, shifting the critical point for phase separation to lower temperatures and reducing the coexistence region in the temperature-concentration plane. A similar suppression is known to occur in equilibrium LLPS upon imposing a uniform external shear [24–27]. The same effect is achieved here via local self-shearing demonstrating that activity provides a new handle for controlling the LLPS phase diagram.

Model.—We consider a phase-separating mixture of a passive isotropic fluid and an active nematic [28]. Such a system has recently been engineered by combining active microtubule nematics with DNA-based condensates [12]. We work in 2D, although the analytical work is easily generalized to 3D. The system is described by three continuum fields: a phase field  $\phi = \langle n_A - n_P \rangle / \langle n_A + n_P \rangle$  that represents the local composition of the fluid mixture, with  $n_{A,P}$  the number density of active and passive particles, a flow velocity **v**, and the nematic order parameter tensor  $Q_{ij} = S/2(n_i n_j - \delta_{ij}/2)$ , where S is the amplitude and **n** the director, with  $|\mathbf{n}| = 1$ . The dynamics is governed by

$$\begin{split} D_t \phi &= M \nabla^2 \mu, \\ D_t Q_{ij} &= \lambda D_{ij} + Q_{ik} \omega_{kj} - \omega_{ik} Q_{kj} - \frac{1}{\gamma} \frac{\delta \mathcal{F}_Q}{\delta Q_{ij}}, \\ \rho D_t v_i &= \eta \nabla^2 v_i - \partial_i P + f_i, \end{split} \tag{1}$$

with  $D_t = \partial_t + v_i \partial_i$ . The field  $\phi$  obeys Cahn-Hilliard dynamics with a mobility M and a chemical potential  $\mu = (\delta \mathcal{F}_{\phi}/\delta \phi)$  obtained from a Landau-Ginzburg (LG) free energy  $\mathcal{F}_{\phi} = \frac{1}{2} \int_{\mathbf{r}} [a\phi^2 + (b/2)\phi^4 + \kappa(\nabla \phi)^2]$ . The parameter a represents the temperature of the passive system and controls the equilibrium critical point  $a_c$  located at  $a_c = 0$  for  $\phi_0 = \int_{\mathbf{r}} \phi(\mathbf{r})/A = 0$ , with A the system area. Considering states of uniform  $\phi(\mathbf{r}) = \bar{\phi}$ , for a > 0 the free energy  $\mathcal{F}_{\phi}$  has a single minimum at  $\bar{\phi} = 0$  corresponding to a uniform (mixed) state. For a < 0, the system minimizes the free energy by demixing into two bulk coexisting states with  $\bar{\phi} = \pm \phi_+ = \pm \sqrt{-a/b}$ . For convenience, we also define  $\tilde{\phi} = (1 + \phi/\phi_+)/2$  so that  $\tilde{\phi} = 1$  corresponds to the active nematic phase and  $\tilde{\phi} = 0$  to the isotropic passive fluid.

The dynamics of the nematic order parameter is controlled by coupling to flow through the symmetrized rate of strain tensor  $D_{ij}=(\partial_i v_j+\partial_j v_i)/2$ , vorticity  $\omega_{ij}=(\partial_i v_j-\partial_j v_i)/2$ , and relaxation controlled by the Landau-de Gennes free energy  $\mathcal{F}_O$  given by

$$\mathcal{F}_{Q} = \frac{1}{2} \int_{\mathbf{r}} \left[ \text{Tr}[\mathbf{Q}^{2}] (\text{Tr}[\mathbf{Q}^{2}] - \tilde{\boldsymbol{\phi}}) + K(\partial_{j} Q_{ik})^{2} \right]. \tag{2}$$

The coupling to  $\tilde{\phi}$  ensures that nematic order does not occur in the passive region, where  $\tilde{\phi} = 0$ .

The flow is governed by a Navier-Stokes equation, with  $\rho$  the constant total density,  $\eta$  the shear viscosity, and P the pressure, fixed by incompressibility  $\nabla \cdot \mathbf{v} = 0$ . The force density  $\mathbf{f}$  has two contributions,  $\mathbf{f} = \mathbf{f}^{\phi} + \mathbf{f}^{Q}$ . The capillary force  $\mathbf{f}^{\phi} = -\phi \nabla \mu$  [29] can be written as the divergence of a deviatoric stress  $\mathbf{f}_{i}^{\phi} = \partial_{j}\sigma_{ij}^{\phi} = -\kappa_{a}\partial_{j}[(\partial_{i}\phi)(\partial_{j}\phi) - \delta_{ij}(\nabla\phi)^{2}/2]$  [30]. We allow for  $\kappa_{a}$  to be different from the stiffness  $\kappa$  in the LG free energy to describe nonequilibrium interfacial stresses akin to active model H [20]. The sign of  $\kappa_{a}$  controls the nature of interfacial active stresses, with  $\kappa_{a} > 0$  and  $\kappa_{a} < 0$  corresponding to stresses that tend to stretch and contract the interface along its length, respectively (see Fig. 1 in the Supplemental Material [31]). As shown previously [20,21],  $\kappa_{a} > 0$  stabilizes the interface, while  $\kappa_{a} < 0$  results in an effective

negative interfacial tension and destabilizes it. The bulk active force  $\mathbf{f}^Q$  is controlled by the liquid crystalline degrees of freedom and is the gradient of the familiar active stress  $f_i^Q = \partial_j \sigma_{ij}^a = \partial_j (\alpha \tilde{\phi} Q_{ij})$  [32]. The coupling to  $\tilde{\phi}$  ensures that the active stress is nonzero only in the nematic phase. The sign of  $\alpha$  controls whether bulk active stresses are contractile ( $\alpha > 0$ ) or extensile ( $\alpha < 0$ ). Related models have been used before to describe coexisting nematic and isotropic phases of active liquid crystals [13–15,33], but the boundary of the coexistence region has not been previously quantified.

Numerical results.—In equilibrium ( $\kappa_a = \kappa$  and  $\alpha = 0$ ), our fluid mixture undergoes bulk phase separation for a < 0. The binodal (coexistence) curve  $a = -\phi_0^2$  and the spinodal curve  $a = -3\phi_0^2$  (we set b = 1) are symmetric inverted parabolas shown in Fig. 1 as solid and dashed black lines, respectively. Below the spinodal parabola, an initially uniform state is unstable to small density fluctuations and phase separates through spinodal decomposition. Between the binodal and spinodal lines, uniform states are metastable, and phase separate through nucleation. Above the binodal line, the uniform state is stable.

Interfacial active stresses alone ( $\kappa_a < 0$  and  $\alpha = 0$ ) narrow the coexistence region, changing the coexistence densities and arresting phase separation, but do not affect the location of the critical point [20,31]. In the following, we focus on the effect of bulk activity and assume

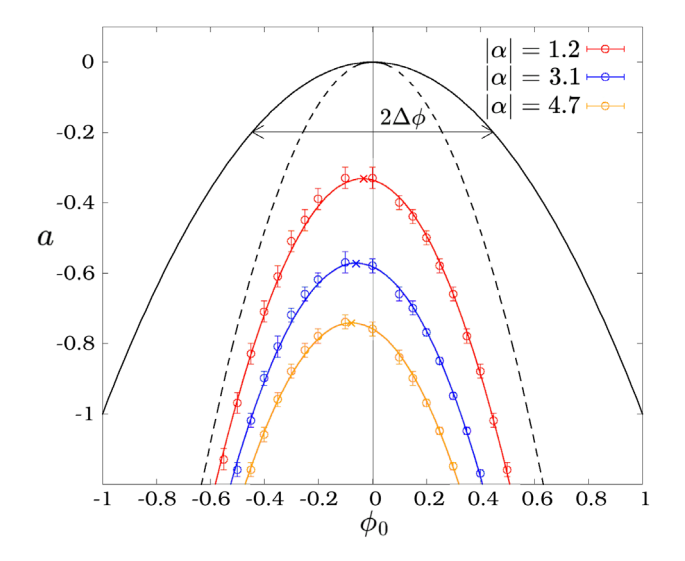


FIG. 1. Phase diagram in the  $(\phi_0,\alpha)$  plane. The black lines are the binodal (solid) and spinodal (dashed) curves for the mean field theory in equilibrium. The numerical data for three values of activity  $\alpha$  clearly show the shift of the critical point and its increase with activity. The lines through the data are parabolic fits and the thick dots mark the critical point. The vertical line at  $\phi_0=0$  highlights the shift of the critical point to values of  $\phi_0$  that correspond to more than 50% of passive fluid. The error bars are the precision with which we can visually differentiate uniform and phase-separated states.

 $\kappa_a = \kappa$  since the effect of  $\kappa_a < 0$  has been discussed elsewhere [20,21].

The situation is completely different in the presence of extensile bulk active stresses ( $\alpha < 0$  and  $\kappa_a = \kappa$ ) that are known to destabilize the uniform ordered state of extensile active nematics for all  $\alpha$  [23]. This instability is driven by bend deformations that grow in time, leading to a dynamical steady state of spatiotemporal chaotic flows known as active turbulence [34]. To quantify the effect of the bulk instability on the phase diagram of the mixture, we integrate numerically Eqs. (1) (see Ref. [31] for details on the numerics). We vary volume fraction  $\phi_0$ , reduced temperature a, and activity  $\alpha$ . The rest of the parameters are as follows, unless specified otherwise:  $\eta = 0.1$ ,  $\gamma = 1$ , K = 0.08,  $\lambda = 1$ , M = 0.1, b = 1,  $\kappa = \kappa_a = 0.7$ .

We find that bulk extensile stresses not only arrest phase separation, but considerably suppress it, by shifting the critical point  $a_c$  to a lower value  $a_c^*(\alpha,\phi_0)<0$  and to  $\phi_0<0$ . The area of the coexistence region in the  $(\phi_0,a)$  plane is substantially reduced, as shown in Fig. 1. To quantify this suppression, we examine the time evolution of the width of the coexistence region  $\Delta\phi(a)=[\max(\phi)-\min(\phi)]/2$  (Fig. 1). In the passive system,  $\Delta\phi(a)=\phi_+=\sqrt{-a}$  with  $\Delta\phi=0$  in the uniform state. The time evolution of  $\Delta\phi$  is shown in the top frame of Fig. 2 for two values of activity, both corresponding to a<0. For  $a_c^*< a<0$ , i.e., above the active critical temperature (a=-0.2, blue curve),  $\Delta\phi$  quickly evolves to zero as the initially phase-separated state is mixed by active flows. For  $a< a_c^*$  (a=-1, red curve), the active fluid evolves toward

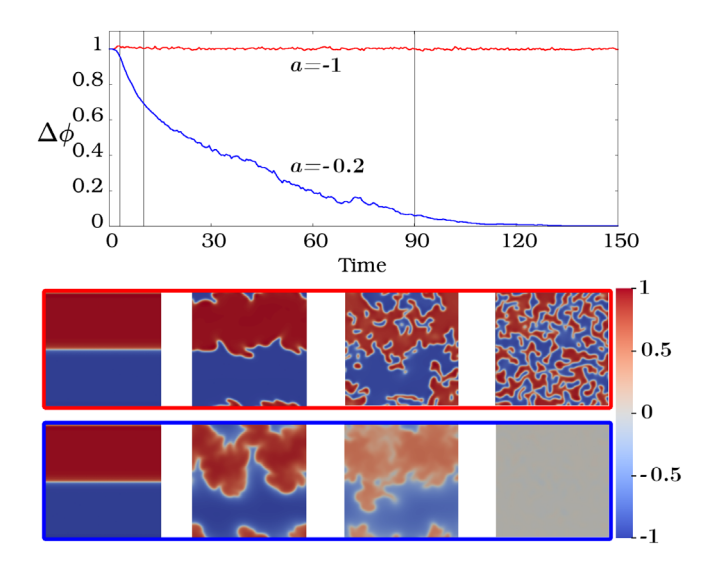


FIG. 2. Top: time evolution of the width  $\Delta\phi$  of the coexistence region for a=-0.2 (blue curve) and a=-1.0 (red curve) corresponding to states above and below the critical point  $a_c^* \approx -0.3$  of the active mixture, respectively. Here,  $|\alpha|=0.8$ . Bottom: snapshots of the simulations at times t=0,3,10, and 90 marked by vertical lines in the plot. The color of the frame of the snapshots matches the color of the corresponding  $\Delta\phi$  curves.

arrested phase separation. The boundaries of the coexistence region shown in Fig. 1 are identified as the points where  $\Delta \phi$  approaches a finite value at late times. We note that this criterion does not distinguish between binodal and spinodal lines.

The active critical point  $a_c^*(\alpha, \phi_0)$  depends on activity and volume fraction. It is shifted downward with increasing activity, which increases the rate at which the mixture is stirred by active energy injection. The parabolic fit to the data in Fig. 1 shows that activity additionally shifts the critical point to lower (negative) values of  $\phi_0$ , which corresponds to mixtures with an excess fraction of active versus passive component.

To determine  $a_c^*(\alpha,\phi_0)$ , we first locate  $\phi_0^c$  through a parabolic fit of the coexistence line, and then evaluate  $\Delta\phi(a,\phi_0^c)$  as a function of a. These curves are shown in the Supplemental Material for several values of activity [31]. The critical point corresponds to  $\Delta\phi(a_c^*,\phi_0^c)=0$  and decreases with increasing activity strength, as evident from Fig. 1 (see also the inset of Fig. 3 in the Supplemental Material [31]). Figure 3 shows a finite-size scaling of  $\Delta\phi(a,\phi_0^c)$  with system size that suggests a continuous phase transition with a diverging  $d\Delta\phi/da$  at the critical point. A system size of L=128 approximates well the asymptotic behavior.

Interfacial dynamics and linear stability.—We show that simple scaling arguments can be used to obtain the growth laws of domains in the coexistence region. To estimate the growth rate of droplets starting from a uniform state, we assume that growth is controlled by a single length scale L

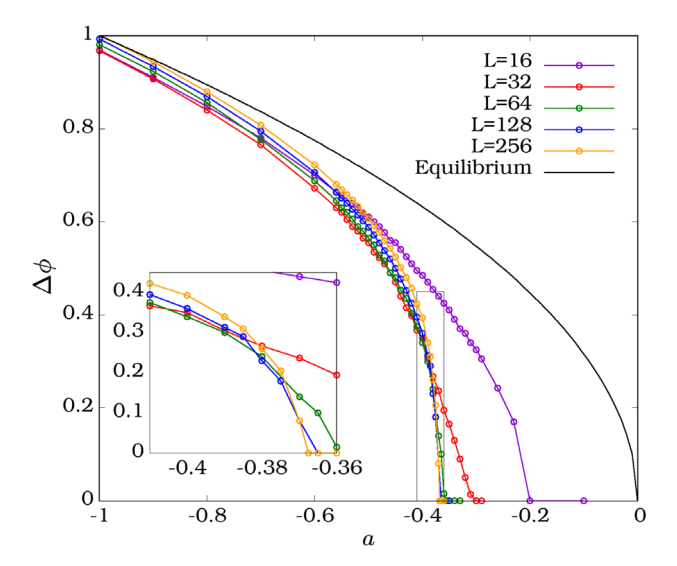


FIG. 3. Finite-size scaling of  $\Delta\phi(a,\phi_c^0)$  for  $|\alpha|=1.2$ . The critical point  $a_c$  is defined as the value of a where  $\Delta\phi=0$ . The black line is the equilibrium mean field line of the passive system, with  $a_c=0$ . For active mixtures,  $a_c$  is shifted to lower (negative) values and approaches  $a_c\approx-0.4$  for the largest system sizes considered.  $d\Delta\phi/da$  diverges at the active critical point. The inset shows an enlarged portion of the data in the black rectangle.

moving at a velocity v so that  $\dot{L} \sim v$ . If the dynamics of the system is dominated by diffusive currents, we estimate  $v \sim \nabla \mu \sim M\sigma/L^2$ , where  $\sigma = [-8\kappa a^3/(9b^2)]^{1/2}$  is the interfacial tension [35]. If the dynamics is dominated by flow, then |v| can be estimated from the Stokes equation by balancing viscous stress with elastic and active stresses as  $\eta v/L^2 \sim \sigma_a/L^2 + \alpha/L + K\lambda/L^3$ , where, for convenience, we have defined an effective active interface tension  $\sigma_a = \kappa_a \sigma/\kappa$ . This active tension arises from interfacial active stresses and can be negative when  $\kappa_a < 0$ , resulting in a self-shearing instability discussed previously in the literature [21]. We can then write the rate of change of L as

$$\dot{L} = s_1 \frac{M\sigma}{L^2} + s_2 \frac{\sigma_a}{\eta} + s_3 \frac{\lambda K}{\eta L} + s_4 \frac{\alpha L}{\eta},\tag{3}$$

where  $s_i$  are unknown constants. For scalar models with no coupling to nematic degrees of freedom, only the first two terms appear in Eq. (3). Active interfacial stresses with  $\sigma_a < 0$  can then arrest coarsening through a self-shearing instability, as discussed in Ref. [21]. This results in domains of typical size  $L^* \sim (M\sigma/|\sigma_a|)^{1/2}$ . When, however, the active fluid is an extensile active nematic, bulk active stresses of strength  $\alpha < 0$  lead to a different path to arrested phase separation. Assuming for simplicity  $\sigma_a = \sigma$ , the first three terms on the right-hand side of Eq. (3) are positive, hence, they describe coarsening, while the last is negative for extensile activity and arrests domain growth.

We can identify three regimes: (i) In the early stages of coarsening, growth is controlled by diffusion of material from smaller to bigger droplets, with  $L(t) \sim t^{1/3}$ . If activity is large enough, growth is arrested at short times when active currents, of order  $j_a \sim \alpha L/\eta$ , balance diffusive currents of order  $j_d \sim M\sigma/L^2$ , resulting in  $L^* \sim \ell_D = (M\sigma\eta/|\alpha|)^{1/3}$ . (ii) At intermediate times, elastic nematic stresses transmit interactions that drive domain growth, with  $L(t) \sim t^{1/2}$ . This mechanism becomes relevant for large nematic stiffness K, resulting in droplets size controlled by the active length  $L^* \sim \ell_a = (K/|\alpha|)^{1/2}$ . (iii) Finally, at late times, drops coalesce through hydrodynamic advection and  $L(t) \sim t$ . In this regime, growth is arrested when interfacial tension balances active stress, which gives  $L^* \sim \ell_\sigma = \sigma/|\alpha|$ .

Whether these regimes are all accessible experimentally depends of course on parameter values. A detailed study of the coarsening dynamics is left for future work. An important prediction, however, is the dependence of the steady state droplet size on activity  $\alpha$ , which may provide a criterion for sorting out the most relevant active mechanisms in experimental realizations.

The scaling arguments presented above are supported by an analysis of the linear stability of a flat interface at y=0. The interfacial height h(x,t) is defined by writing the phase field as  $\phi(r,t)=f(y+h(x,t))$ , such that f(u) changes sharply at u=0, i.e.,  $f'(u)\approx \delta(u)$ . We assume that the

active fluid occupying the region y>0 is in an initial uniform nematic state aligned with the interface, justified because extensile active nematics tend to align with interfaces through a process called active anchoring [13,36]. We can then write  $Q_{xx}\approx S(u)/2$  and  $Q_{xy}\approx S(u)\theta(x,t)$ , where S(u) is the amplitude of the nematic order parameter, with  $S'(u)\approx\delta(u)$ , and  $\theta(x,t)$  the small angle of the nematic director with respect to the interface. We eliminate the velocity  $v_i$  by assuming low Reynolds number and solving for the Stokes flow by imposing incompressibility. The Fourier components of the velocity are  $v_i(\mathbf{q},t)=P_{ij}(\mathbf{q})f_j(q,t)/\eta q^2$ , with  $P_{ij}(\mathbf{q})=\delta_{ij}-\hat{q}_i\hat{q}_j$  a projection operator and  $\hat{q}_i=q_i/|\mathbf{q}|$ . Following Refs. [29,37], we can then obtain linear equations for  $h(q_x,t)$  and  $\theta(q_x,t)$  given by [31]

$$\partial_t \binom{h}{\theta} = A \binom{h}{\theta} \tag{4}$$

with

$$A = \begin{bmatrix} -\frac{\sigma_a |q_x|}{4\eta} - \frac{M\sigma |q_x|^3}{2} & -\frac{\alpha i q_x}{2\eta q_x^2} \\ \frac{\kappa_a \sigma |q_x| i q_x}{4\kappa \eta} + \frac{\alpha (1-\lambda) i q_x}{8\eta} & -\frac{\alpha \lambda}{2\eta} - \frac{K}{\gamma} q_x^2 \end{bmatrix}.$$
 (5)

For  $\alpha=0$ , height and director fluctuations are decoupled. Height fluctuations become unstable for  $\sigma_a<0$  below a wave number  $q^*\sim \sqrt{|\sigma_a|/(\sigma\eta M)}$ , signaling arrested phase separation with structures of size  $L^*\sim 2\pi/q^*$ . Bulk extensile activity ( $\alpha<0$ ) destabilizes director fluctuations on all

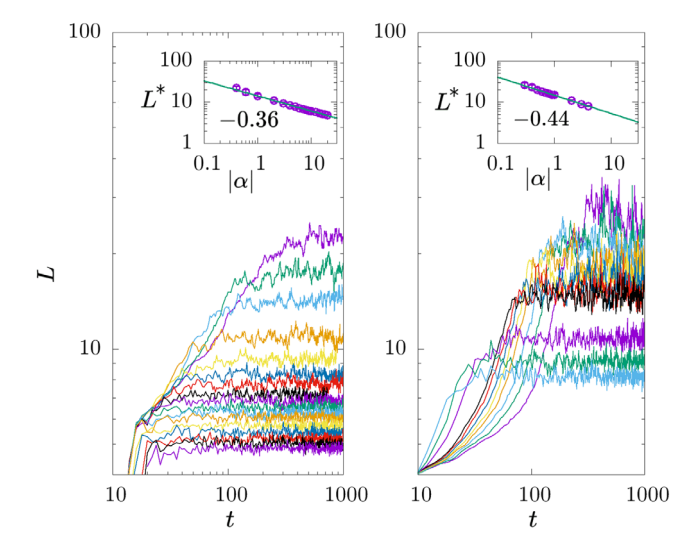


FIG. 4. Droplet size as a function of the time for an initially uniform state and various activity for two sets of parameters. Left:  $l_D \approx 10 l_\alpha$  (left), i.e., regime (i) where coarsening is controlled by diffusion and we estimate  $L^* \sim |\alpha|^{-1/3}$ . Right:  $l_\alpha \approx 10 l_D$  (right), i.e., regime (ii) where coarsening is controlled by elasticity and we estimate  $L^* \sim |\alpha|^{-1/2}$ . The insets show the scaling of the saturation value  $L^*$  with  $|\alpha|$ .

scales according to the generic instability of bulk active nematics [23]. When  $\sigma_a > 0$ , the coupling to interfacial relaxation can stabilize the nematic above a characteristic length scale, often in a regime where the modes become complex, signaling the propagation of surface waves similar to capillary waves in inertial fluids [1,38].

A detailed analysis is presented in the Supplemental Material [31]. As expected on the basis of scaling arguments,  $q^*$  is controlled by the three active length scales (for  $\sigma_a = \sigma$ )  $\ell_D$ ,  $\ell_a$ ,  $\ell_\sigma$ , with crossovers between the three scalings with increasing activity. Figure 4 shows the growth in time of droplet size in the microphase-separated state for various activities, and the scaling of  $L^*$  with activity (inset) for two set of parameters corresponding to regimes (i) and (ii).

In summary, we have shown that interfacial and bulk active stresses play distinct roles in the LLPS of active and passive mixtures. Previously studied interfacial stresses can arrest the phase separation via a shearing instability of the interface, but do not affect the location of the critical point. This is because their action is confined at the interface, where the concentration gradients are finite. In contrast, bulk extensile active stresses can suppress phase separation entirely by sustained self-stirring of the active component. As a result, bulk active stresses can significantly shift the critical point of the passive phase-separating mixture to lower temperatures and shrink the size of the coexistence region in the volume fraction-temperature plane. Within the coexistence region, phase separation is arrested leading to an emulsion steady state of dynamic droplets that continuously coalesce and split due to the shear flows created by the active nematic.

Our Letter quantifies the role of activity on the phase diagram of phase-separating active-passive binary mixtures. It highlights the distinct roles of interfacial and bulk active stresses, and it shows that bulk active stresses coupling to liquid crystalline degrees of freedom can shift the critical point. Our results on the scaling of the typical droplet size as a function of the activity in the dynamical emulsion offer quantitative criteria for discerning the mechanisms that arrest phase separation in experiments and simulations.

We thank Zhihong You, Cesare Nardini, Alexandra Tayar, and Zvonimir Dogic for illuminating discussions. This work was supported by NSF Grant No. DMR-2041459.

- fmc36@ucsb.edu
- [1] R. Adkins, I. Kolvin, Z. You, S. Witthaus, M. C. Marchetti, and Z. Dogic, Science 377, 768 (2022).
- [2] A. Doostmohammadi, J. Ignés-Mullol, J. M. Yeomans, and F. Sagués, Nat. Commun. 9, 3246 (2018).
- [3] J. Tailleur and M. E. Cates, Phys. Rev. Lett. **100**, 218103 (2008).

- [4] Y. Fily and M. C. Marchetti, Phys. Rev. Lett. 108, 235702 (2012).
- [5] G. S. Redner, M. F. Hagan, and A. Baskaran, Phys. Rev. Lett. 110, 055701 (2013).
- [6] M. E. Cates and J. Tailleur, Annu. Rev. Condens. Matter Phys. 6, 219 (2015).
- [7] J. Stenhammar, D. Marenduzzo, R. J. Allen, and M. E. Cates, Soft Matter 10, 1489 (2014).
- [8] Y. Fily, S. Henkes, and M. C. Marchetti, Soft Matter 10, 2132 (2014).
- [9] F. Caballero, C. Nardini, and M. E. Cates, J. Stat. Mech. (2018) 123208.
- [10] J. Palacci, S. Sacanna, A. P. Steinberg, D. J. Pine, and P. M. Chaikin, Science 339, 936 (2013).
- [11] V. Narayan, S. Ramaswamy, and N. Menon, Science 317, 105 (2007).
- [12] A. M. Tayar, M. F. Hagan, and Z. Dogic, Proc. Natl. Acad. Sci. U.S.A. 118, e2102873118 (2021).
- [13] M. L. Blow, S. P. Thampi, and J. M. Yeomans, Phys. Rev. Lett. 113, 248303 (2014).
- [14] R. Hughes and J. M. Yeomans, Phys. Rev. E **102**, 020601(R) (2020).
- [15] L. Giomi and A. DeSimone, Phys. Rev. Lett. 112, 147802 (2014).
- [16] S. Williams, R. Jeanneret, I. Tuval, and M. Polin, Nat. Commun. 13, 4776 (2022).
- [17] G. Xu, T. Huang, Y. Han, and Y. Chen, Soft Matter 17, 9607 (2021).
- [18] P. M. Chaikin, T. C. Lubensky, and T. A. Witten, *Principles of Condensed Matter Physics* (Cambridge University Press, Cambridge, England, 1995), Vol. 10.
- [19] R. Wittkowski, A. Tiribocchi, J. Stenhammar, R. J. Allen, D. Marenduzzo, and M. E. Cates, Nat. Commun. 5, 4351 (2014).
- [20] A. Tiribocchi, R. Wittkowski, D. Marenduzzo, and M. E. Cates, Phys. Rev. Lett. **115**, 188302 (2015).
- [21] R. Singh and M. E. Cates, Phys. Rev. Lett. **123**, 148005 (2019).
- [22] E. Tjhung, C. Nardini, and M. E. Cates, Phys. Rev. X 8, 031080 (2018).
- [23] R. A. Simha and S. Ramaswamy, Phys. Rev. Lett. 89, 058101 (2002).
- [24] C. C. Han, Y. Yao, R. Zhang, and E. K. Hobbie, Polymer **47**, 3271 (2006).
- [25] A. Onuki, J. Phys. Condens. Matter 9, 6119 (1997).
- [26] A. Onuki, Intl. J. Therm. Phys. 16, 381 (1995).
- [27] A. Silberberg and W. Kuhn, Nature (London) **170**, 450 (1952).
- [28] The model can be adapted to describe a mixture of active and passive nematic by decoupling the  $Tr[\mathbf{Q}^2]$  term in the free energy from  $\phi$ , while maintaining the coupling to  $\phi$  in the active stress.
- [29] A. J. Bray, A. Cavagna, and R. D. M. Travasso, Phys. Rev. E 65, 016104 (2001).
- [30] M. E. Cates and E. Tjhung, J. Fluid Mech. **836**, P1 (2018).
- [31] See Supplemental Material at http://link.aps.org/supplemental/10.1103/PhysRevLett.129.268002 for details.
- [32] M. C. Marchetti, J. F. Joanny, S. Ramaswamy, T. B. Liverpool, J. Prost, M. Rao, and R. A. Simha, Rev. Mod. Phys. 85, 1143 (2013).

- [33] R. C. V. Coelho, N. A. M. Araújo, and M. M. Telo da Gama, Soft Matter 18, 7642 (2022).
- [34] R. Alert, J. Casademunt, and J.-F. Joanny, Annu. Rev. Condens. Matter Phys. 13, 143 (2022).
- [35] V. M. Kendon, M. E. Cates, I. Pagonabarraga, J.-C. Desplat, and P. Bladon, J. Fluid Mech. 440, 147 (2001).
- [36] R. C. V. Coelho, N. A. M. Araújo, and M. M. T. da Gama, Phil. Trans. R. Soc. A **379** (2021).
- [37] G. Fausti, E. Tjhung, M. E. Cates, and C. Nardini, Phys. Rev. Lett. **127**, 068001 (2021).
- [38] H. Soni, W. Luo, R. A. Pelcovits, and T. R. Powers, Soft Matter 15, 6318 (2019).